

---

# Visual Transformers: Token-based Image Representation and Processing for Computer Vision

---

Bichen Wu<sup>1</sup>, Chenfeng Xu<sup>2</sup>, Xiaoliang Dai<sup>1</sup>, Alvin Wan<sup>1</sup>,  
Peizhao Zhang<sup>1</sup>, Masayoshi Tomizuka<sup>2</sup>, Kurt Keutzer<sup>2</sup>, Peter Vajda<sup>1</sup>  
<sup>1</sup>Facebook, <sup>2</sup>UC Berkeley  
{wbc,xiaoliangdai,stzpz,vajdap}@fb.com,  
{xuchenfeng,alvinwan,tomizuka,keutzer}@berkeley.edu

## Abstract

Computer vision has achieved great success using standardized image representations – pixel arrays, and the corresponding deep learning operators – convolutions. In this work, we challenge this paradigm: we instead (a) represent images as a set of visual tokens and (b) apply *visual transformers* to find relationships between visual semantic concepts. Given an input image, we dynamically extract a set of visual tokens from the image to obtain a compact representation for high-level semantics. We then use visual transformers to operate over the visual tokens to densely model relationships between them. We find that this paradigm of token-based image representation and processing drastically outperforms its convolutional counterparts on image classification and semantic segmentation. To demonstrate the power of this approach on ImageNet classification, we use ResNet as a convenient baseline and use visual transformers to replace the last stage of convolutions. This reduces the stage’s MACs by up to 6.9x, while attaining up to 4.53 points higher top-1 accuracy. For semantic segmentation, we use a visual-transformer-based FPN (VT-FPN) module to replace a convolution-based FPN, saving 6.5x fewer MACs while achieving up to 0.35 points higher mIoU on LIP and COCO-stuff.

## 1 Introduction

In modern digital imaging and computer vision, visual information is captured and processed as arrays of pixels: a 2D image is represented as a 3D array. The *de facto* deep learning operator for computer vision, convolutional filters, accepts and outputs 3D pixel arrays. Although convolving over pixel arrays has achieved great success, there are critical limitations:

- 1) **Not all pixels are created equal:** For the target task, each pixel has varying importance. For example, image classification models should prioritize foreground objects over background. Additionally, semantic segmentation models should prioritize miniscule pedestrians over disproportionately large swaths of sky, road, vegetation etc. Despite this, convolutions uniformly distribute computation over all pixels, regardless of importance. This leads to redundancy in both computation and representation.
- 2) **Convolutions struggle with capturing long-range interactions:** Each convolutional filter is constrained to operate on a small (e.g.,  $3 \times 3$ ) region due to computational cost quadratic in kernel size. However, long-range interactions between semantic concepts is vital, as evidenced by large numbers of context-driven work using operations like dilations and global average pooling. However, these are only temporary fixes for the underlying pixel-convolution issue.
- 3) **Convolutions are not efficient for sparse, high-level semantic concepts:** Low-level visual features such as corners and edges are densely distributed across images; as a result, convolutions are apt for image processing early in a neural network. However, as the receptive field increases deeper

in the network, the number of potential patterns grows exponentially large. As a result, semantic concepts become increasingly sparse: each concept appears in small regions of a few images. Later convolutions become correspondingly inefficient.

We propose a new paradigm that overcomes the above limitations and achieves better performance (accuracy) with lower computational cost on vision tasks. More specifically, our intuition is to replace pixel arrays with language-like descriptors: A sentence with several words (i.e., tokens) suffices to describe an image. Unlike pixel arrays, such token-based representations are compact. We thus propose *visual transformers* to: (a) re-represent images with visual tokens and (b) process tokens with transformers (i.e., self-attention). The visual transformer is illustrated in Figure 1: We first convolve over the input image, then re-represent the feature map as a small number of visual, semantic tokens. We then apply a cascaded set of transformers, a self-attention module widely used in natural language processing [1] to process visual tokens, capture interactions, and compute output tokens. These tokens are directly used for image-level prediction tasks such as image classification. For pixel-level prediction tasks like semantic segmentation, we project the output tokens back to the feature map and use the aggregated feature map.

To demonstrate this idea we use visual transformers to replace convolution-based modules in baseline vision models. Experiments show that using visual transformers achieve higher accuracy with lower computational cost on classification tasks on ImageNet [2] and show similar advantages on the semantic segmentation task on COCO-Stuff [3] and Look-Into-Person [4] datasets. On ImageNet, we use ResNet[5] as a convenient baseline to enable comparison and replace the last stage with visual transformers, saving up to 6.9x MACs for the stage and achieving up to 4.53 points higher top-1 accuracy. ResNet34 using visual transformers can outperform ResNet101 using 2.5x fewer MACs. For semantic segmentation, we use visual-transformers to re-design the feature-pyramid networks (FPN) and save 6.4x MACs while achieving higher mIoU on LIP and COCO-Stuff datasets.

## 2 Related work

**Attention in vision models:** Attention is an effective mechanism recently added to the deep learning toolbox. It has been widely used in natural language processing [1, 6] and is gaining popularity in computer vision [7–18]. Attention was first used to modulate the feature map: some attention values are computed from the input and multiplied to the feature map as in [9, 7, 8, 10]. Later work [11, 19, 20] interpret this “modulation” as a way to make convolution spatially adaptive and content-aware. In [12], Wang *et al.* introduced self-attention, also called non-local operators, to video understanding and use it to capture the long-range interactions. However, self-attention in computer vision is computationally expensive since the complexity grows quadratically with the number of pixels. [16] use self-attention to augment convolutions and reduce the compute cost by using small channel sizes for attention. [18, 13, 21, 17, 15] on the other hand restrict receptive field of self-attention and use it in a convolutional manner. Since [18], self-attentions are used as a stand-alone building block for vision models. Our work is different from all above since we are the first to challenge the paradigm of pixel array-based image representation.

**Efficient vision models:** Many recent research efforts have been focusing on building vision models to achieve better performance using lower computational cost. Early work [22, 23] achieves this by carefully choosing convolutional layers with smaller kernel and channel size, the following work [24–29] explores new variations of convolution operators. Recently, people begin to use neural architecture search [30–34] to optimize network’s performance and efficiency within a predefined search space that consists of existing convolution-based operators. After years’ of progress, it is becoming increasingly hard to further improve vision models under the current paradigm. Our work seek a new angle to this problem and aim to eliminate the redundancy in the vision representation and processing based on pixel-arrays and convolutions.

## 3 Visual transformer

In this section, we introduce the details of the visual transformer. The overall diagram of a visual transformer is illustrated in Figure 1. For a given image, we first use convolutions to extract a feature map representation, since convolutions are very effective processing low-level visual features. We feed the feature maps into stacked visual transformers. Each visual transformer consists of three

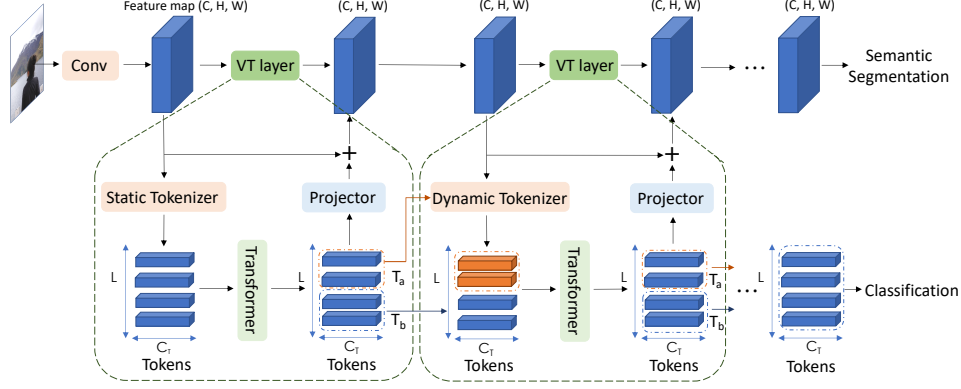


Figure 1: Diagram of a visual transformer.

major components: a tokenizer, a transformer, and a projector. The tokenizer extracts a small number of visual tokens from the feature map, the transformer captures the interaction between the visual tokens and computes the output tokens, and the projector fuses the output tokens back to the feature map. Through out the visual transformers, we keep both visual tokens and feature maps as output since visual tokens capture high-level semantics in the image while the feature map preserves the pixel-level details. Since the computations are performed only on a small number of visual tokens, the computational cost for the visual transformer is very low. At the end of the network, we use visual tokens for image-level prediction tasks, such as image classification, and use the accumulated feature map for pixel-level prediction tasks, such as semantic segmentation. The pseudo-code implementation for key components of visual transformer can be found in Appendix A.

### 3.1 Extracting visual tokens

#### 3.1.1 Static tokenization

First we discuss how do we extract visual tokens from a feature map, as illustrated in Figure 2a. Each visual token represents a semantic concept in the image, and we compute visual tokens by spatially aggregating the feature map. Formally, a feature map can be represented by  $X \in \mathbf{R}^{H \times W \times C}$ , where  $H, W$  are the height and width of the feature map,  $C$  is the channel size. For notation convenience, we denote  $\bar{X} \in \mathbf{R}^{HW \times C}$  as a reshaped matrix of  $X$  by merging the two spatial dimensions into one. Visual tokens can be represented by  $T \in \mathbf{R}^{L \times C_T}$  where  $L$  is the number of visual tokens,  $L \ll (HW)$ .  $C_T$  is the channel size of a visual token. We compute visual tokens as

$$T = \text{softmax}(\bar{X}W_A^T)(\bar{X}W_V) = A^TV = \sum_i A[i, :]^T V[i, :]. \quad (1)$$

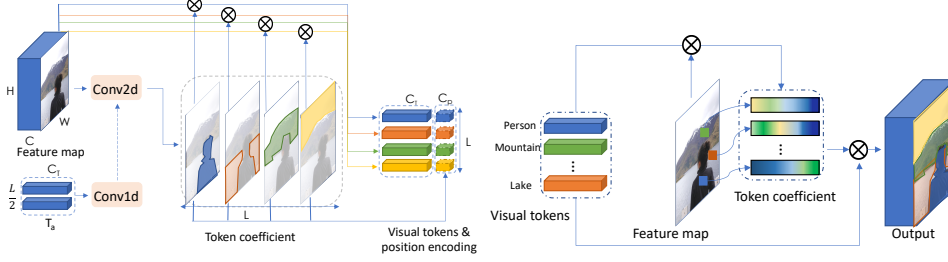
$W_V \in \mathbf{R}^{C \times C_T}$  is a learnable weight to convert the feature map  $X$  into  $V \in \mathbf{R}^{HW \times C_T}$ . This step can be implemented as a point-wise 2D convolution. Visual tokens can be seen as a weighted average of the feature map.  $A \in \mathbf{R}^{HW \times L}$  is a normalized token coefficient, and the value of  $A[i, l] \in \mathbf{R}$  determines the contribution of the  $i$ -th pixel  $V[i, :]$  to the  $l$ -th token  $T[l, :]$ .  $W_A \in \mathbf{R}^{L \times C}$  is the weight we use to compute  $A$ . It can be seen as a convolutional filter that divides the feature map  $X$  into various regions that corresponds to different semantic concepts. This is illustrated in Figure 2a. The visualization of the token coefficients  $A$  on real images can be found in Figure 5.

#### 3.1.2 Position encoding

Visual tokens are computed as a weighted average from the original feature map, but equation (1) does not encode the contribution from individual pixels so the position of each visual token is lost. Intuitively, position information is important to understand the image semantics. This information is recorded in the token coefficient  $A \in \mathbf{R}^{HW \times L}$ . To encode positions, we compute

$$P = \text{downsample}(A)^T W_{A \rightarrow P}. \quad (2)$$

We first downsample  $A$  spatially to the size of  $(\bar{H}\bar{W}, L)$ , and multiply it with a learnable weight  $W_{A \rightarrow P} \in \mathbf{R}^{\bar{H}\bar{W} \times C_p}$  to compress the position information in  $A$  to a smaller encoding vector with



(a) Diagram of a tokenizer. It uses a static or a dynamic weight to group the pixels into tokens with back to the feature map. Through attention, each different semantic concepts. Position encodings pixel decides how to combine information from are computed from the token coefficients. visual tokens.

Figure 2: Diagram of a tokenizer and a projector.

dimension  $C_p$ . Then, we augment the visual tokens  $T \in \mathbf{R}^{L \times C_T}$  by concatenating position encoding  $P \in \mathbf{R}^{L \times C_p}$  along the channel dimension to include the positional information. We can optionally use another 1D convolution to adjust the channel size of the concatenated visual tokens.

### 3.2 Transformer

Visual tokens extracted from the feature map do not have intrinsic orders between them, so unlike pixel-arrays, we cannot use convolutions (except point-wise convolutions) to process them. So instead we use transformers, which can process sets of elements. Formally, a transformer can be described as

$$T_{out} = T_{in} + (\text{softmax}((T_{in}K)(T_{in}Q)^T)(T_{in}V))F, \quad (3)$$

where  $T_{in}, T_{out} \in \mathbf{R}^{L \times C_T}$  is the input and output tokens.  $K \in \mathbf{R}^{C_T \times C_T/2}$ ,  $Q \in \mathbf{R}^{C_T \times C_T/2}$ ,  $V \in \mathbf{R}^{C_T \times C_T}$ ,  $F \in \mathbf{R}^{C_T \times C_T}$  are learnable weights used to compute keys, queries, values, and output tokens. The computational cost for equation (3) is  $3C_T^2L + 1.5L^2C_T$ , where  $3C_T^2L$  is to compute keys, queries, values, output tokens,  $1.5L^2C_T$  is for multiplying keys, queries, and values.

Note that transformer (self-attention) has been used in computer vision and is also referred as the “non-local” operation. A non-local operation can also be described by equation (3). However, for non-local operations, instead of operating on visual tokens, they directly operate on the entire feature map  $X \in \mathbf{R}^{H \times W \times C}$ . As a consequence, the computational cost under the same configuration is  $3HWC^2 + 1.5(HW)^2C$ . To provide a concrete example, assume  $H = W = 7, C = 512$ . A non-local operator will require 40.3 million MACs. In our experiment, a visual transformer with  $L = 8$  tokens are sufficient to achieve better results, but the computational cost for the transformer is 6.3 million, or 6.4x smaller than the non-local operation on the pixel array.

### 3.3 Fusing visual tokens with the feature map

Many vision tasks require pixel-level details, but such details are not preserved in the visual tokens. Therefore, we fuse the output of transformer back to the feature map to augment the pixel-level representation. To achieve this, we compute

$$\bar{X}_{out} = \bar{X}_{in} + \text{softmax}((\bar{X}_{in}Q_{T \rightarrow X})(T_{out}K_{T \rightarrow X})^T)(T_{out}V_{T \rightarrow X}). \quad (4)$$

Here  $Q_{T \rightarrow X} \in \mathbf{R}^{C_T \times C}$  is a learnable weight used to compute queries from the input feature map. The queries decide the information a pixel needs from the visual tokens.  $K_{T \rightarrow X} \in \mathbf{R}^{C_T \times C}$  is a learnable weight to compute keys from the visual tokens, and the keys encode the information each visual token contains.  $V_{T \rightarrow X} \in \mathbf{R}^{C_T \times C}$  is a learnable weight to compute the values from the visual token that will be fused with the feature map. The intuition is illustrated in Figure 2b.

### 3.4 Dynamic tokenization

Same as convolution, we cascade layers of visual transformers together so each layer takes the previous layer’s visual tokens and feature maps as input. Within each layer, in order to capture more semantic concepts from the feature map, we use equation (1) to extract new visual tokens and combine with the existing ones. However, instead of using  $W_A$  as a static weight, we dynamically

compute  $W_A$  from the input visual tokens. With a static weight, we extract a fixed set of semantic concepts regardless of the input image. However, high-level semantics in images are very sparse and diverse, exceeding the capacity of a small set of fixed filters. So instead, we compute  $W_A$  based on the previous visual tokens. With the input token  $T_{in} \in \mathbf{R}^{L, C_T}$ , we first split it along the token dimension to obtain  $T_{in,a}, T_{in,b} \in \mathbf{R}^{L/2, C_T}$ , and we update the visual tokens as

$$T'_{in} = \text{concat}_L(T_{in,b}, \text{tokenizer}(T_{in,a}W_{T \rightarrow W_A}, X_{in})). \quad (5)$$

$\text{tokenizer}(\cdot, \cdot)$  is a function defined by equation (1) that extract visual tokens from the feature map  $X_{in}$  using a point-wise 2D convolutional filter  $(T_{in,a}W_{T \rightarrow W_A}) \in \mathbf{R}^{L/2, C}$ .  $W_{T \rightarrow W_A} \in \mathbf{R}^{C_T \times C}$  is a learnable weight that generates the filter based on the input visual token  $T_{in,a}$ . Then, we concatenate the new tokens with  $T_{in,b}$  to get  $T'_{in} \in \mathbf{R}^{L \times C_T}$  and feed it to the transformer, as shown in Figure 1.

## 4 Using visual transformers to build vision models

Now that we have discussed the basics of visual transformers, we discuss how to use visual transformers as building blocks for vision models. We use three hyper-parameters to control a block of visual transformer: channel size of the output feature map  $C$ , channel size of visual token  $C_T$ , and the number of visual tokens  $L$ . In a series of cascaded visual transformers, the first block accepts a feature map as input. If the channel size of the input feature map is not the same as visual transformer, we simply use a point-wise 2D convolution on the input feature map to adjust the channel size. For the first visual transformer block, we use static tokenization and in later blocks, we use dynamic tokenization. If the visual token’s channel size  $C_T$  is not the same as the input feature’s channel size  $C$ , we simply apply a point-wise 1D convolution to adjust the channel size. Following previous work [1, 18], we use multi-head attention in the tokenizer, transformer, and projector. To further reduce the computational complexity, we use group convolutions to reduce the MACs and parameter sizes. To provide more details, We provide pseudo code for the visual transformer Appendix A. We will also open-source the model after the paper publication.

### 4.1 Visual transformers for image classification

For image classification, we build our networks with backbones inherited from ResNet [5], since its simple and elegant architecture makes it an ideal baseline to demonstrate new ideas. Based on ResNet- $\{18, 34, 50, 101\}$ , we build corresponding visual-transformer-ResNets (VT-ResNet). For all the models, we keep stage-1 through stage-4 from the original ResNet the same and use them to extract feature maps. We replace the last stage of the network with visual transformer blocks. On the ImageNet dataset, all the models accept input images with a resolution of  $224 \times 224$  so the output of stage-4 is a feature map with a resolution of  $14 \times 14$ . Visual transformers take this as the input, and extract  $L=8$  visual tokens with channel size  $C_T = 1024$ . We set the output feature map’s channel size as 512 for VT-ResNet- $\{18, 34\}$  and 1024 for VT-ResNet- $\{50, 101\}$ . At the end of the network, we output 8 visual tokens and feed it to the classification head. A table summarizing the stage-wise description of the model is provided in Appendix B.

### 4.2 Visual transformers for semantic segmentation

We hypothesize that using visual transformers as a building block for semantic segmentation can offer several challenges over convolutions. First, the computational complexity of convolution grows quadratically with the image resolution. Second, convolutions struggles to capture long-term interactions between pixels. Visual transformers, on the other hand, operate on a small number of visual tokens regardless of the image resolution, and since it computes interactions between semantic concepts, it bypasses the “long-range” challenge with pixel-arrays.

To verify this, we use panoptic feature pyramid networks (FPN) [35] as a baseline and use visual transformers to improve the network. Panoptic FPN offers a simple, strong, and open-source baseline to demonstrate new ideas. Panoptic FPNs use ResNet as backbones to extract feature maps from different stages with various resolutions. These feature maps are then fused by a feature pyramid network in a top-down manner to generate a multi-scale and detail preserving feature map with rich semantics for segmentation. This is illustrated in Figure 3. FPN is computationally expensive since it heavily relies on spatial convolutions operating on high resolution feature maps with large

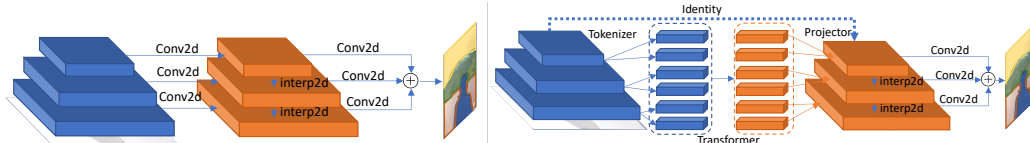


Figure 3: Feature Pyramid Networks (FPN) (left) vs visual-transformer-FPN (VT-FPN) (right) for semantic segmentation.

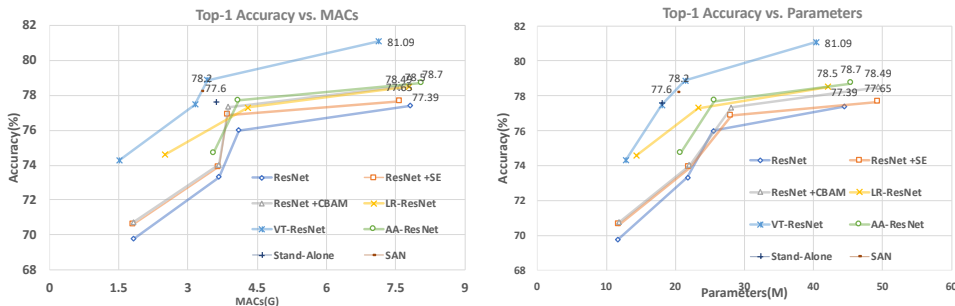


Figure 4: Accuracy vs. MACs and parameters for visual transformer and related work on ImageNet.

channel sizes. Therefore, we use visual transformers to replace the convolutions in FPN. We name the new module as VT-FPN, which is shown in Figure 3. From each feature map, VT-FPN extract  $L=8$  visual tokens with a channel size  $CT=1024$ . The visual tokens are combined and fed into one transformer to compute to capture interactions between visual tokens from different resolutions. The output tokens are then projected back to the original feature maps, which are then used to perform pixel-level prediction. Compared with the original FPN based on convolution, the computational cost for VT-FPN is much smaller since we only operate on a very small number of visual tokens rather than all the pixels. Instead of fusing feature maps pixels by pixels via convolution and interpolation, we use a transformer to fuse feature maps globally. Our experiment shows VT-FPN uses 6.5x fewer MACs than FPN while preserving or surpassing its performance.

## 5 Experiments

### 5.1 ImageNet classification

For image classification, we conduct experiments on the ImageNet dataset [2]. We implement VT-ResNets in Pytorch and train them on the ImageNet training set with around 1.3 million images and evaluate on the validation set. We train the models for 400 epochs with RMSProp. We use an initial learning rate of 0.01 and increase it to 0.16 in 5 warmup epochs, then reduce the learning rate by a factor of 0.9875 per epoch. We use synchronized batch normalization and distributed training with a batch size of 2048. We use label smoothing and AutoAugment [36] in the training. Additionally, we set the stochastic depth survival probability [37] and dropout ratio to be 0.9 and 0.2, respectively. We use exponential moving average (EMA) on the model weights with a decay of 0.99985.

Our results are reported in Table 1 and Figure 4. The baseline ResNet models are based on the references from Pytorch: [https://pytorch.org/hub/pytorch\\_vision\\_resnet/](https://pytorch.org/hub/pytorch_vision_resnet/). Compared with the baseline ResNet models, VT-ResNet models achieved up to 4.84 points higher accuracy with fewer MACs and parameters. Note that the parameter and MAC reduction is the result of only replacing one stage of the baseline model. If we consider the reduction over the original stage, the MAC reduction is up to 6.9x, as shown in Table 2. It is our future work to study how to replace more stages of convolutions. We compare our results with other previous methods [7, 9, 16, 38, 15, 18, 17] that adopt attention in different ways on ResNets. Figure 4 shows our models significantly outperform all previous ones with higher accuracy and lower MACs and parameter sizes.

### 5.2 Ablation study

We introduce many new components in a visual transformer. We conduct ablation studies to examine the role of several key components. To accelerate the experiment, we only train VT-ResNet-{18, 34} for 90 epochs. We verify the role of the following components in a visual transformer. 1) Transformer:

Table 1: Experiments of visual-transformer-based ResNets on the ImageNet dataset. R-18 denotes ResNet-18. VT-R-18 denotes visual-transformer-ResNet-18. \*The baseline MACs reported in [9] is lower than this work.  $\Delta$  MACs calculated based on the baseline in [9].

Models	Top-1 Acc (%)	$\Delta$ Top-1 Acc (%)	MACs (G)	$\Delta$ MACs (M)	Params (M)	$\Delta$ Params (M)
R-18 [5]	69.76	-	1.814	-	<b>11.67</b>	-
R-18 + SE [7, 9]	70.59	+0.83	1.814	+0	11.78	+0.11
R-18 + CBAM [9]	70.73	+0.97	1.815	+1	11.78	+0.11
LR-R-18 [15]	<b>74.6</b>	<b>+4.84</b>	2.5	+686	14.4	+2.62
VT-R-18 (ours)	74.29	+4.53	<b>1.587</b>	<b>-227</b>	12.76	+1.09
R-34 [5]	73.32	-	3.664	-	21.78	-
R-34 + SE [7, 9]	73.87	+0.55	3.664	0	21.96	+0.18
R-34 + CBAM [9]	74.01	+0.69	3.664	0	21.96	+0.18
AA-R-34 [16]	74.7	+1.38	3.55	-224	20.7	-1.08
VT-R-34 (ours)	<b>77.46</b>	<b>+4.14</b>	<b>3.151</b>	<b>-513</b>	<b>18.02</b>	<b>-3.76</b>
R-50 [5]	76.0	-	4.089	-	25.5	-
R-50 + SE [7, 9]	76.86	+0.86	3.860*	+2*	28.1	+2.6
R-50 + CBAM [9]	77.34	+1.34	3.864*	+6*	28.1	+2.6
LR-R-50 [15]	77.3	+1.3	4.3	+211	23.3	-2.2
Stand-Alone [18]	77.6	+1.6	3.6	-489	<b>18.0</b>	<b>-7.5</b>
AA-R-50 [16]	77.7	+1.7	4.1	+11	25.6	+0.1
A <sup>2</sup> -R-50 [38]	77.0	+1.0	-	-	-	-
SAN19 [17]	78.2	+2.2	<b>3.3</b>	<b>-789</b>	20.5	-5
VT-R-50 (ours)	<b>78.88</b>	<b>+2.88</b>	3.412	-677	21.4	-4.1
R-101 [5]	77.39	-	7.802	-	44.44	-
R-101 + SE [7, 9]	77.65	+0.26	7.575*	+5*	49.33	+4.89
R-101 + CBAM [9]	78.49	+1.10	7.581*	+11*	49.33	+4.89
LR-R-101 [15]	78.5	+1.11	7.79	-12	42.0	-2.44
AA-R-101 [16]	78.7	+1.31	8.05	+248	45.4	+0.96
VT-R-101 (ours)	<b>81.09</b>	<b>+3.70</b>	<b>7.127</b>	<b>-675</b>	<b>40.33</b>	<b>-4.11</b>

Table 2: MAC and parameter size reduction of visual transformers on ResNets.

		R18	R34	R50	R101
MACs	Total	1.14x	1.16x	1.20x	1.09x
	Stage-5	2.4x	5.0x	6.1x	6.9x
Params	Total	0.91x	1.21x	1.19x	1.19x
	Stage-5	0.9x	1.5x	1.26x	1.26x

we use transformers to capture interaction between visual tokens, which we hypothesize is important for understanding the image semantics. To verify this, we replace the transformer with a point-wise 1D convolution. It shows the accuracy drops by 1.96% and 0.32% without transformers. 2) We hypothesize dynamic tokenization can better deal with the sparse semantic concepts. To verify this, we replaced all the dynamic tokenization with static ones, and our experiment shows the accuracy drops by 1.19% and 1.25%. 3) We hypothesize that position encoding is important for understanding semantic concepts. After removing the position encoding, the accuracy drops by 0.02% and 0.15%.

Table 3: Ablation studies on VT-ResNet. “-TF” denotes removing transformers, “-PE”: removing position encoding, “-DT”: removing dynamic tokenization, “Base”: baseline.

Model	Ablation	Top-1 Acc (%)	MACs (G)	Params (M)
VT-R-18	Base	71.45	1.587	12.76
	- TF	69.49 (-1.96)	1.519	8.57
	- PE	71.43 (-0.02)	1.586	12.69
	- DT	70.26 (-1.19)	1.608	12.22
VT-R-34	Base	74.65	3.217	18.02
	- TF	74.33 (-0.32)	3.204	17.24
	- PE	74.50 (-0.15)	3.216	17.90
	- DT	73.40 (-1.25)	3.246	16.92

### 5.3 Visual transformers for semantic segmentation

We conduct experiments to test the effectiveness of visual transformer for semantic segmentation on the COCO-stuff dataset [3] and the LIP dataset [4]. COCO-stuff dataset contains annotations for 91 stuff classes with 118K training images and 5K validation images. LIP dataset is a collection of images containing human appearing with challenging poses and views. For COCO-stuff dataset, we train a VT-FPN model with ResNet- $\{50, 101\}$  backbones. Our implementation is based on Detectron2 [39]. Our training recipe is based on the semantic segmentation FPN recipe with 1x training steps, except that we use synchronized batch normalization in the VT-FPN, change the batch size to 32, and use a base learning rate of 0.04. For the LIP dataset, we also use synchronized batch normalization with a batch size of 96. We optimize the model via SGD with weight decay of 0.0005 and learning rate of 0.01. Our models and the training recipes will be open-sourced after the paper publication.

As we can see in Table 4, after replacing FPN with VT-FPN, both ResNet-50 and ResNet-101 based models achieve slightly higher mIoU, but VT-FPN requires 6.5x fewer MACs than FPNs, demonstrating the effectiveness of visual transformer.

Table 4: Semantic segmentation results on the COCO-stuff validation set and the LIP validation set. The MACs for COCO-stuff is calculated with a typical input resolution of  $800 \times 1216$  and the MACs for LIP is calculated with an input resolution of  $473 \times 473$ .

		mIoU (%)	Total MACs (G)	FPN MACs (G)	Dataset
R-50	FPN	40.78	159	55.1	COCO-stuff
	VT-FPN	41.00	113 (1.41x)	8.5 (6.48x)	
	FPN	47.04	37.1	12.8	LIP
	VT-FPN	47.39	26.4 (1.41x)	2.0 (6.40x)	
R-101	FPN	41.51	231	55.1	COCO-stuff
	VT-FPN	41.50	185 (1.25x)	8.5 (6.48x)	
	FPN	47.35	54.4	12.8	LIP
	VT-FPN	47.58	43.6 (1.25x)	2.0 (6.40x)	

### 5.4 Visualizations of visual tokens

We hypothesize that visual tokens extracted in the visual transformer correspond to different high-level semantics in the image. To better understand this, we visualize the token coefficients  $A \in \mathbf{R}^{H \times W \times L}$ , where each  $A[:, l] \in \mathbf{R}^{H \times W}$  is an attention map to show how each part of the image contributes to token- $l$ . We plot the attention map in Figure 5, and we can see that without any supervision, different visual tokens are attending to different semantic concepts in the image corresponding to parts of the background or foreground objects. More visualization results are provided in Appendix C.

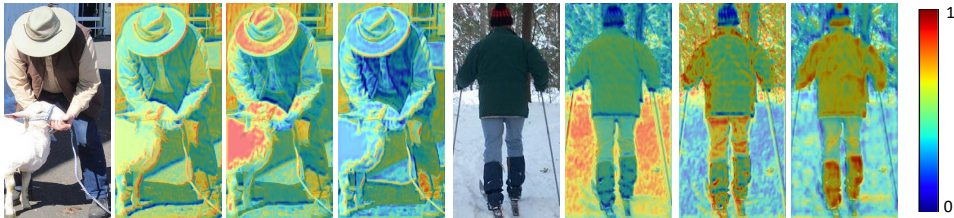


Figure 5: Token coefficient visualization from the LIP dataset. Red pixels have larger token coefficients and blue ones have smaller. Although without supervision, different visual tokens selectively focus on different regions such as snow grounds, forest, sheep, and person.

## 6 Conclusions

In this paper, we propose visual transformers to challenge the existing computer vision paradigm that represents and processes images with pixel arrays and convolutions. Visual transformers overcome the limitations of the existing paradigm by representing an image with a compact set of dynamically extracted visual tokens and densely modeling their interactions with transformers. We use visual transformers to replace convolution-based modules in vision models and we observe significant accuracy and efficiency improvement in image classification and semantic segmentation. For example,

ResNet34 using visual transformers can outperform ResNet101 while using 2.5x fewer MACs, visual transformer-based FPN uses 6.5x fewer MACs than regular FPNs while achieving similar accuracy.

## **7 Broader impact discussion**

Our primary goal for this work is to advance the scientific understanding of vision systems. The scientific questions we hope to answer through this paper include 1) How to build vision systems to efficiently represent and process semantic concepts; 2) How to bridge the low-level perception to high-level reasoning vision systems. We answer these questions by building and experimenting a new vision paradigm and testing it on several vision tasks. Our experiment show that our proposed paradigm can achieve significantly better performance on several existing vision tasks while being more computationally efficient. This provides us with promising results to help us better answer the scientific questions above. In addition, the practical impact of our work is that it can help us build better and more efficient vision systems for many applications including AR/VR, autonomous driving, medical imaging, robotics, and so on. Our method is generic and we sincerely hope it will be used for purposes that are beneficial to our society. However, like any many other technologies, there are risks that the method proposed in this paper can be used for no-so-beneficial purposes. Given the generic nature of this paper, it is hard for us to predict specific bad applications using this method. However, as researchers, we hope that by publishing this paper so everyone can access it, we can increase the chance that the research community as a whole will collectively supervise its applications and make sure it is used for the common good.

## References

- [1] Ashish Vaswani, Noam Shazeer, Niki Parmar, Jakob Uszkoreit, Llion Jones, Aidan N Gomez, Łukasz Kaiser, and Illia Polosukhin. Attention is all you need. In *Advances in neural information processing systems*, pages 5998–6008, 2017.
- [2] Jia Deng, Wei Dong, Richard Socher, Li-Jia Li, Kai Li, and Li Fei-Fei. Imagenet: A large-scale hierarchical image database. In *2009 IEEE conference on computer vision and pattern recognition*, pages 248–255. Ieee, 2009.
- [3] Holger Caesar, Jasper Uijlings, and Vittorio Ferrari. Coco-stuff: Thing and stuff classes in context. In *Computer vision and pattern recognition (CVPR), 2018 IEEE conference on*. IEEE, 2018.
- [4] Xiaodan Liang, Ke Gong, Xiaohui Shen, and Liang Lin. Look into person: Joint body parsing & pose estimation network and a new benchmark. *IEEE transactions on pattern analysis and machine intelligence*, 41(4):871–885, 2018.
- [5] Kaiming He, Xiangyu Zhang, Shaoqing Ren, and Jian Sun. Deep residual learning for image recognition. In *Proceedings of the IEEE conference on computer vision and pattern recognition*, pages 770–778, 2016.
- [6] Jacob Devlin, Ming-Wei Chang, Kenton Lee, and Kristina Toutanova. Bert: Pre-training of deep bidirectional transformers for language understanding. *arXiv preprint arXiv:1810.04805*, 2018.
- [7] Jie Hu, Li Shen, and Gang Sun. Squeeze-and-excitation networks. In *Proceedings of the IEEE conference on computer vision and pattern recognition*, pages 7132–7141, 2018.
- [8] Jie Hu, Li Shen, Samuel Albanie, Gang Sun, and Andrea Vedaldi. Gather-excite: Exploiting feature context in convolutional neural networks. In *Advances in Neural Information Processing Systems*, pages 9401–9411, 2018.
- [9] Sanghyun Woo, Jongchan Park, Joon-Young Lee, and In So Kweon. Cbam: Convolutional block attention module. In *Proceedings of the European Conference on Computer Vision (ECCV)*, pages 3–19, 2018.
- [10] Bichen Wu, Xuanyu Zhou, Sicheng Zhao, Xiangyu Yue, and Kurt Keutzer. Squeezesegv2: Improved model structure and unsupervised domain adaptation for road-object segmentation from a lidar point cloud. In *ICRA*, 2019.
- [11] Chenfeng Xu, Bichen Wu, Zining Wang, Wei Zhan, Peter Vajda, Kurt Keutzer, and Masayoshi Tomizuka. Squeezesegv3: Spatially-adaptive convolution for efficient point-cloud segmentation. *arXiv preprint arXiv:2004.01803*, 2020.
- [12] Xiaolong Wang, Ross Girshick, Abhinav Gupta, and Kaiming He. Non-local neural networks. In *Proceedings of the IEEE conference on computer vision and pattern recognition*, pages 7794–7803, 2018.
- [13] Niki Parmar, Ashish Vaswani, Jakob Uszkoreit, Łukasz Kaiser, Noam Shazeer, Alexander Ku, and Dustin Tran. Image transformer. *arXiv preprint arXiv:1802.05751*, 2018.
- [14] Han Hu, Jiayuan Gu, Zheng Zhang, Jifeng Dai, and Yichen Wei. Relation networks for object detection. In *Proceedings of the IEEE Conference on Computer Vision and Pattern Recognition*, pages 3588–3597, 2018.
- [15] Han Hu, Zheng Zhang, Zhenda Xie, and Stephen Lin. Local relation networks for image recognition. In *Proceedings of the IEEE International Conference on Computer Vision*, pages 3464–3473, 2019.
- [16] Irwan Bello, Barret Zoph, Ashish Vaswani, Jonathon Shlens, and Quoc V Le. Attention augmented convolutional networks. In *Proceedings of the IEEE International Conference on Computer Vision*, pages 3286–3295, 2019.

- [17] Hengshuang Zhao, Jiaya Jia, and Vladlen Koltun. Exploring self-attention for image recognition. *arXiv preprint arXiv:2004.13621*, 2020.
- [18] Prajit Ramachandran, Niki Parmar, Ashish Vaswani, Irwan Bello, Anselm Levskaya, and Jonathon Shlens. Stand-alone self-attention in vision models. *arXiv preprint arXiv:1906.05909*, 2019.
- [19] Hang Su, Varun Jampani, Deqing Sun, Orazio Gallo, Erik Learned-Miller, and Jan Kautz. Pixel-adaptive convolutional neural networks. In *Proceedings of the IEEE Conference on Computer Vision and Pattern Recognition (CVPR)*, 2019.
- [20] Weiyue Wang and Ulrich Neumann. Depth-aware cnn for rgb-d segmentation. In *Proceedings of the European Conference on Computer Vision (ECCV)*, pages 135–150, 2018.
- [21] Jean-Baptiste Cordonnier, Andreas Loukas, and Martin Jaggi. On the relationship between self-attention and convolutional layers. *arXiv preprint arXiv:1911.03584*, 2019.
- [22] Forrest N Iandola, Song Han, Matthew W Moskewicz, Khalid Ashraf, William J Dally, and Kurt Keutzer. Squeezenet: Alexnet-level accuracy with 50x fewer parameters and < 0.5 mb model size. *arXiv preprint arXiv:1602.07360*, 2016.
- [23] Amir Gholami, Kiseok Kwon, Bichen Wu, Zizheng Tai, Xiangyu Yue, Peter Jin, Sicheng Zhao, and Kurt Keutzer. Squeezenext: Hardware-aware neural network design. In *Proceedings of the IEEE Conference on Computer Vision and Pattern Recognition Workshops*, pages 1638–1647, 2018.
- [24] Andrew G Howard, Menglong Zhu, Bo Chen, Dmitry Kalenichenko, Weijun Wang, Tobias Weyand, Marco Andreetto, and Hartwig Adam. Mobilenets: Efficient convolutional neural networks for mobile vision applications. *arXiv preprint arXiv:1704.04861*, 2017.
- [25] Mark Sandler, Andrew Howard, Menglong Zhu, Andrey Zhmoginov, and Liang-Chieh Chen. Mobilenetv2: Inverted residuals and linear bottlenecks. In *Proceedings of the IEEE conference on computer vision and pattern recognition*, pages 4510–4520, 2018.
- [26] Andrew Howard, Mark Sandler, Grace Chu, Liang-Chieh Chen, Bo Chen, Mingxing Tan, Weijun Wang, Yukun Zhu, Ruoming Pang, Vijay Vasudevan, et al. Searching for mobilenetv3. In *Proceedings of the IEEE International Conference on Computer Vision*, pages 1314–1324, 2019.
- [27] Xiangyu Zhang, Xinyu Zhou, Mengxiao Lin, and Jian Sun. Shufflenet: An extremely efficient convolutional neural network for mobile devices. In *Proceedings of the IEEE conference on computer vision and pattern recognition*, pages 6848–6856, 2018.
- [28] Ningning Ma, Xiangyu Zhang, Hai-Tao Zheng, and Jian Sun. Shufflenet v2: Practical guidelines for efficient cnn architecture design. In *Proceedings of the European Conference on Computer Vision (ECCV)*, pages 116–131, 2018.
- [29] Bichen Wu, Alvin Wan, Xiangyu Yue, Peter Jin, Sicheng Zhao, Noah Golmant, Amir Gholaminejad, Joseph Gonzalez, and Kurt Keutzer. Shift: A zero flop, zero parameter alternative to spatial convolutions. In *Proceedings of the IEEE Conference on Computer Vision and Pattern Recognition*, pages 9127–9135, 2018.
- [30] Bichen Wu, Xiaoliang Dai, Peizhao Zhang, Yanghan Wang, Fei Sun, Yiming Wu, Yuandong Tian, Peter Vajda, Yangqing Jia, and Kurt Keutzer. Fbnet: Hardware-aware efficient convnet design via differentiable neural architecture search. In *Proceedings of the IEEE Conference on Computer Vision and Pattern Recognition*, pages 10734–10742, 2019.
- [31] Xiaoliang Dai, Peizhao Zhang, Bichen Wu, Hongxu Yin, Fei Sun, Yanghan Wang, Marat Dukhan, Yunqing Hu, Yiming Wu, Yangqing Jia, et al. Chamnet: Towards efficient network design through platform-aware model adaptation. In *Proceedings of the IEEE Conference on Computer Vision and Pattern Recognition*, pages 11398–11407, 2019.

- [32] Alvin Wan, Xiaoliang Dai, Peizhao Zhang, Zijian He, Yuandong Tian, Saining Xie, Bichen Wu, Matthew Yu, Tao Xu, Kan Chen, et al. Fbnetv2: Differentiable neural architecture search for spatial and channel dimensions. *arXiv preprint arXiv:2004.05565*, 2020.
- [33] Mingxing Tan and Quoc V Le. Efficientnet: Rethinking model scaling for convolutional neural networks. *arXiv preprint arXiv:1905.11946*, 2019.
- [34] Mingxing Tan, Bo Chen, Ruoming Pang, Vijay Vasudevan, Mark Sandler, Andrew Howard, and Quoc V Le. Mnasnet: Platform-aware neural architecture search for mobile. In *Proceedings of the IEEE Conference on Computer Vision and Pattern Recognition*, pages 2820–2828, 2019.
- [35] Alexander Kirillov, Ross Girshick, Kaiming He, and Piotr Dollár. Panoptic feature pyramid networks. In *Proceedings of the IEEE Conference on Computer Vision and Pattern Recognition*, pages 6399–6408, 2019.
- [36] Ekin D Cubuk, Barret Zoph, Dandelion Mane, Vijay Vasudevan, and Quoc V Le. Autoaugment: Learning augmentation strategies from data. In *Proceedings of the IEEE conference on computer vision and pattern recognition*, pages 113–123, 2019.
- [37] Gao Huang, Yu Sun, Zhuang Liu, Daniel Sedra, and Kilian Q Weinberger. Deep networks with stochastic depth. In *European conference on computer vision*, pages 646–661. Springer, 2016.
- [38] Yunpeng Chen, Yannis Kalantidis, Jianshu Li, Shuicheng Yan, and Jiashi Feng. A<sup>2</sup>-nets: Double attention networks. In *Advances in Neural Information Processing Systems*, pages 352–361, 2018.
- [39] Yuxin Wu, Alexander Kirillov, Francisco Massa, Wan-Yen Lo, and Ross Girshick. Detectron2. <https://github.com/facebookresearch/detectron2>, 2019.

## A Pseudo-code implementation of visual transformers

In this section, we provide the pseudo-code for key components of visual transformer. Note that the pseudo-code is just to help readers understand visual transformer. To make this easier to understand, we remove many important implementation details, such as normalization and initialization, so this is not a rigorous implementation that guarantees reproducibility. We will open-source our model and code implementation afterwards.

The pseudo-code for the static and dynamic tokenizer described in Section 3.1.1 and 3.4.

```
1 class Tokenizer(nn.Module):
2     def __init__(self, L, CT, C, head=16, groups=16, dynamic=False):
3         super(Tokenizer, self).__init__()
4         if not dynamic
5             # use static weights to compute token coefficients.
6             self.conv_token_coef = conv1x1_2d(C, L)
7         else:
8             # use previous tokens to compute a query weight, which is
9             # then used to compute token coefficients.
10            self.conv_query = conv1x1_1d(CT, C)
11            self.conv_key = conv1x1_2d(C, C, groups=groups)
12            self.conv_value = conv1x1_2d(C, C, groups=groups)
13            self.pos_encoding = PosEncoder()
14            self.conv_token = conv1x1_1d(
15                C + self.pos_encoding.pos_dim, CT)
16            self.head = head
17            self.dynamic = dynamic
18
19     def forward(self, feature, token):
20         # compute token coefficients
21         #feature: N, C, H, W, token: N, CT, L
22         if not self.dynamic
23             token_coef = self.conv_token_coef(feature)
24             N, L, H, W = token_coef.shape
25             token_coef = token_coef.view(N, 1, L, H * W)
26             token_coef = token_coef.permute(0, 1, 3, 2) # N, 1, HW, L
27             token_coef = token_coef / np.sqrt(feature.shape[1])
28         else:
29             L = token.shape[2]
30             # Split input tokens
31             # T_a, T_b: N, CT, L//2
32             T_a, T_b = tokens[:, :, :L // 2], tokens[:, :, L // 2:]
33             query = self.conv_query(T_a)
34             N, C, L_a = query.shape
35             # N, h, C//h, L_a
36             query = query.view(N, self.head, C // self.head, L_a)
37             N, C, H, W = feature.shape
38             key = self.conv_key(feature).view(
39                 N, self.head, C // self.head, H * W) # N, h, C//h, HW
40             # Compute token coefficients.
41             # N, h, HW, L_a
42             token_coef = torch.matmul(key.permute(0, 1, 3, 2), query)
43             token_coef = token_coef / np.sqrt(C / self.head)
44             N, C, H, W = feature.shape
45             token_coef = F.softmax(token_coef, dim=2)
46             value = self.conv_value(feature).view(
47                 N, self.head, C // self.head, H * W) # N, h, C//h, HW
48             # extract tokens from the feature map
49             # static tokens: N, C, L. dynamic tokens: N, C, L_a
50             tokens = torch.matmul(value, token_coef).view(N, C, -1)
51             # compute position encoding
52             # if static: pos_encoding: N, Cp, L else: N, Cp, L_a
53             pos_encoding = self.pos_encoding(token_coef, (H, W))
54             tokens = torch.cat((tokens, pos_encoding), dim=1)
55         if not self.dynamic
```

```

56     # N, C+Cp, L -> N, CT, L
57     tokens = self.conv_token(tokens)
58     else:
59     # N, C+Cp, L_a -> N, CT, L_a, then cat to N, CT, (L_a + L_b)
60     tokens = torch.cat((T_b, self.conv_token(tokens)), dim=2)
61     return tokens

```

Listing 1: Pseudo-code of the tokenizer.

The pseudo-code implementation for the position encoder, described in Section 3.1.2.

```

1 class PosEncoder(nn.Module):
2     def __init__(self, C, size, num_downsample):
3         super(PosEncoder, self).__init__()
4         self.size = size
5         ds_conv = []
6         for _ in range(num_downsample):
7             ds_conv.append(conv3x3_2d(dim, dim, stride=2))
8         ds_conv.append(conv1x1_2d(dim, 1))
9         self.ds_conv = nn.Sequential(*ds_conv)
10        pos_dim = size**2 // (4**num_downsample)
11        self.pos_conv = conv1x1_1d(pos_dim, pos_dim)
12        self.pos_dim = pos_dim
13
14    def forward(self, token_coef, input_size):
15        H, W = input_size
16        N, h, HW, L = token_coef.shape
17        token_coef = token_coef.view(N * L, h, H, W)
18        # interpolation to deal with input with varying sizes
19        token_coef = F.interpolate(
20            token_coef, size=(self.size, self.size))
21        # downsampling
22        token_coef = self.ds_conv(token_coef)
23        token_coef = token_coef.view(N, L, -1).permute(0, 2, 1)
24        # compress and compute the position encoding.
25        return self.pos_conv(token_coef) # N, Cp, L

```

Listing 2: Pseudo-code of the position encoder.

The pseudo-code implementation for the transformer, described in Section 3.2.

```

1 class Transformer(nn.Module):
2     def __init__(self, CT, head=16, kqv_groups=8):
3         super(Transformer, self).__init__()
4         self.k_conv = conv1x1_1d(CT, CT // 2, groups=kqv_groups)
5         self.q_conv = conv1x1_1d(CT, CT // 2, groups=kqv_groups)
6         self.v_conv = conv1x1_1d(CT, CT, groups=kqv_groups)
7         self.ff_conv = conv1x1_1d(CT, CT)
8         self.head = head
9         self.CT = CT
10
11    def forward(self, tokens):
12        N = tokens.shape[0]
13        # k: N, h, CT//2//h, L
14        k = self.k_conv(tokens).view(
15            N, self.head, self.CT // 2 // self.head, -1)
16        # q: N, h, CT//2//h, L
17        q = self.q_conv(tokens).view(
18            N, self.head, self.CT // 2 // self.head, -1)
19        # v: N, h, CT//h, L
20        v = self.v_conv(tokens).view(
21            N, self.head, self.CT // self.head, -1)
22        # kq: N, h, L, L
23        kq = torch.matmul(k.permute(0, 1, 3, 2), q)
24        kq = F.softmax(kq / np.sqrt(kq.shape[2]), dim=2)
25        # kqv: N, CT, L

```

```

26     kqv = torch.matmul(v, kq).view(N, self.CT, -1)
27     tokens = tokens + kqv
28     tokens = tokens + self.ff_conv(tokens)
29     return tokens

```

Listing 3: Pseudo-code of the transformer.

The pseudo-code implementation for the projector, described in Section 3.3.

```

1 class Projector(nn.Module):
2     def __init__(self, CT, C, head=16, groups=16):
3         super(Projector, self).__init__()
4         self.proj_value_conv = conv1x1_1d(CT, C)
5         self.proj_key_conv = conv1x1_1d(CT, C),
6         self.proj_query_conv = conv1x1_2d(C, CT, groups=groups)
7         self.head = head
8
9     def forward(self, feature, token):
10        N, _, L = token.shape
11        h = self.head
12        proj_v = self.proj_value_conv(token).view(N, h, -1, L)
13        proj_k = self.proj_key_conv(token).view(N, h, -1, L)
14        proj_q = self.proj_query_conv(feature)
15        N, C, H, W = proj_q.shape
16        proj_q = proj_q.view(N, h, C // h, H * W).permute(0, 1, 3, 2)
17        # proj_coef: N, h, HW, L
18        proj_coef = F.softmax(
19            torch.matmul(proj_q, proj_k) / np.sqrt(C / h), dim=3)
20        # proj: N, h, C//h, HW
21        proj = torch.matmul(proj_v, proj_coef.permute(0, 1, 3, 2))
22        _, _, H, W = x.shape
23        proj = .view(N, -1, H, W))
24        return feature + proj.view(N, -1, H, W)

```

Listing 4: Pseudo-code of the projector.

## B Stage-wise model description of VT-ResNet

In this section, we provide a detailed description of the model configurations for visual-transformer-based ResNet (VT-ResNet). We use three hyper-parameters to control a block of visual transformer: channel size of the output feature map  $C$ , channel size of visual token  $CT$ , and the number of visual tokens  $L$ . The model configurations of VT-ResNets are described in Table 5.

Table 5: Model descriptions for VT-ResNets. VT-R-18 denotes visual-transformer-ResNet-18. “conv7×7-C64-S2” denotes a 7-by-7 convolution with an output channel size of 64 and a stride of 2. “BB-C64×2” denotes a basic block [5] with an output channel size of 64 and it is repeated twice. “BN-C256×3” denotes a bottleneck block [5] with an output channel size of 256 and it is repeated by three times. “VT-C512-L8-CT1024×2” denotes a visual transformer block with a channel size for the output feature map as 512, channel size for visual tokens as 1024, and the number of tokens as 8.

Stage	Resolution	VT-R-18	VT-R-34	VT-R-50	VT-R-101
1	56×56	conv7×7-C64-S2 → maxpool3×3-S2			
2	56×56	BB-C64×2	BB-C64×3	BN-C256×3	BN-C256×3
3	28×28	BB-C128×2	BB-C128×4	BN-C512×4	BN-C512×4
4	14×14	BB-C256×2	BB-C256×6	BN-C1024×6	BN-C1024×23
5	14×14    8	VT-C512-L8 -CT1024×2	VT-C512-L8 -CT1024×3	VT-C1024-L8 -CT1024×3	VT-C1024-L8 -CT1024×3
head	8	avgpool-fc1000			

## C More visualization results

We provide more visualization of the token coefficients in Figure 6.



Figure 6: Token coefficient visualization. Color red denotes higher coefficient values and color blue denotes lower coefficient values. From the visualization, we can see that without any supervision, visual tokens automatically focus on different areas of the image that correspond to different semantic concepts. This supports our intuition of how visual tokens work.